

Deformation-based vulnerability functions for RC bridges

A.S. Elnashai†

*CEE Department, 205 North Mathews Avenue, University of Illinois at Urbana-Champaign,
Urbana, Illinois 61801, USA*

B. Borzi‡

EQE International Ltd., UK

S. Vlachos‡

Thomi Engineering, Athens, Greece

(Received April 13, 2003, Accepted October 1, 2003)

Abstract. There is an ever-increasing demand for assessment of earthquake effects on transportation structures, emphasised by the crippling consequences of recent earthquakes hitting developed countries reliant on road transportation. In this work, vulnerability functions for RC bridges are derived analytically using advanced material characterisation, high quality earthquake records and adaptive inelastic dynamic analysis techniques. Four limit states are employed, all based on deformational quantities, in line with recent development of deformation-based seismic assessment. The analytically-derived vulnerability functions are then compared to a data set comprising observational damage data from the Northridge (California 1994) and Hyogo-ken Nanbu (Kobe 1995) earthquakes. The good agreement gives some confidence in the derived formulation that is recommended for use in seismic risk assessment. Furthermore, by varying the dimensions of the prototype bridge used in the study, and the span lengths supported by piers, three more bridges are obtained with different overstrength ratios (ratio of design-to-available base shear). The process of derivation of vulnerability functions is repeated and the ensuing relationships compared. The results point towards the feasibility of deriving scaling factors that may be used to obtain the set of vulnerability functions for a bridge with the knowledge of a ‘generic’ function and the overstrength ratio. It is demonstrated that this simple procedure gives satisfactory results for the case considered and may be used in the future to facilitate the process of deriving analytical vulnerability functions for classes of bridges once a generic relationship is established.

Key words: vulnerability functions; RC bridges; seismic response; damage assessment.

† Willett Professor, Acting Director of Mid-America Earthquake Center

‡ Senior Engineer

1. Introduction and preliminaries

1.1 Significance of bridge structures

Transportation networks are vital for the development of modern societies and hence their integrity must be protected. Bridges are the most sensitive elements of a transportation system. The closure of a bridge that represents the only or most important link between two areas separated by water or other geological feature would potentially lead to severe consequences for industry, commerce and society as a whole. If the economic loss due to closure of a main arterial bridge is assessed alongside the cost of seismic retrofitting of the structure, the case for assessment and re-design of bridge structures in seismic areas will be immediately apparent. It is therefore of priority to re-assess bridge structures in areas subjected to appreciable seismic hazard with a view to estimate and minimise earthquake damage. In this respect, the use of vulnerability functions, i.e. relationships between a ground motion parameter and the probability of a limit state being exceeded, assumes an important role.

Accepting the limitations of deriving vulnerability functions from observations, the objective of this study is to analytically derive vulnerability curves for reinforced concrete bridges based on deformational limit states. Whereas it is appreciated that comparing vulnerability curves for a specific structure with observational data for a wide range of bridges is not theoretically meaningful, the results of this procedure are compared with the limited available empirically-derived vulnerability curves to establish a degree of confidence in the derivation. Moreover vulnerability assessment of bridges would be significantly simplified if a procedure to approximate vulnerability curves of reinforced concrete bridges, with the same basic configuration, were available. Towards this objective, the relationship between vulnerability curves of different bridges with similar basic configuration is examined. Finally, the possibility of parametrising bridge vulnerability functions in terms of structural response is explored with some success.

1.2 Assessment techniques for seismic safety

The seismic vulnerability of a civil engineering facility is the probability that a given intensity of earthquake input will cause a limit state criterion to be achieved or exceeded. Vulnerability studies are in general undertaken employing relationships that express the probability of damage as a function of a ground motion parameter, since neither the input motion nor the structural behaviour can be described deterministically. The two widely used forms of motion-versus-damage relationships are vulnerability curves and damage probability matrices (DPM). A plot of the computed conditional probability versus the ground motion parameter is defined as the vulnerability curve for the damage state, whilst the discrete probability of reaching or exceeding a damage state for a certain input motion severity represents an element of the DPM. The damage level is randomly described corresponding to random input variables. Out of the large number of parameters, which affect the behaviour of structures under seismic action, only those considered to influence significantly the response are assumed as random variable. The principal steps for the evaluation of vulnerability curves and DPMs are:

- i. identification of random input variables and hence likely scenarios of systems based on a prototype structure;
- ii. quantification of potential ground motion;

- iii. evaluation of structural response;
- iv. comparison between demand, corresponding to the seismic hazard, and limit states of the considered structural system.

Vulnerability analyses may be either empirical or analytical depending on whether observational or analytical results are utilised, respectively. In the first case the information available on structures similar to those for which the seismic vulnerability is sought must be selected (e.g. Basöz *et al.* 1999, Yamazaki *et al.* 1999, both for bridges, Rossetto and Elnashai 2003 for buildings, amongst others). A flow chart of the analytical definition of vulnerability curves and DPMs is represented in Fig. 1.

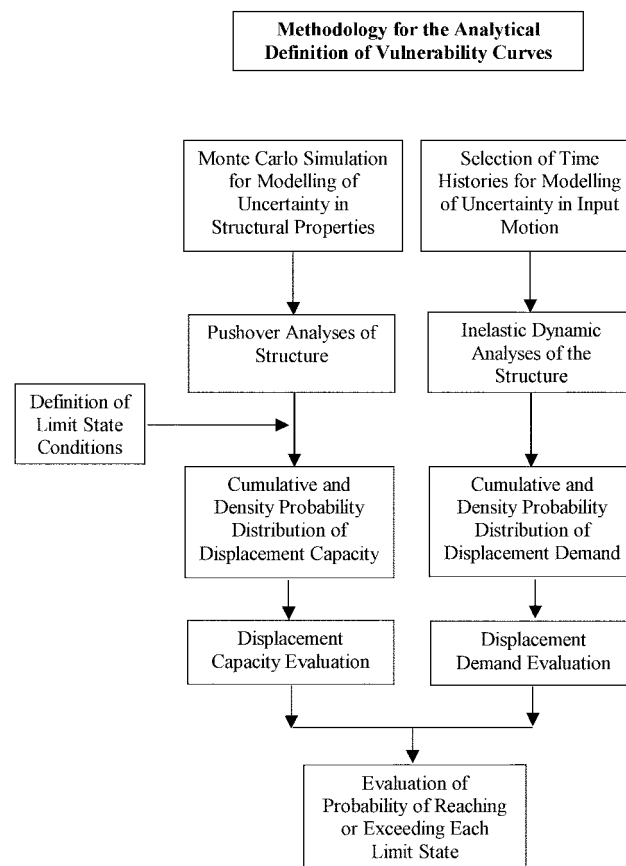


Fig. 1 Flow chart for the analytical evaluation of Vulnerability Curves

1.3 Review of vulnerability assessment methods for bridges

RC bridges, like other structural forms, may be grouped according to the characteristics that are deemed to influence their seismic response (e.g. foundation system, bent configuration, deck-pier connection, deck type, abutment type etc). Bridges in the same class are expected to exhibit similar seismic performance and damage levels under a given earthquake scenario. Special care should be taken in grouping bridges into classes, as an extremely detailed classification may lead to extreme

complexity of applications. This is inconsistent with the expected errors in probabilistically-derived vulnerability curves, especially when comparing analytical curves to field observations.

When vulnerability curves are analytically derived, they represent the behaviour of a prototype structure and material dispersions thereof, hence the need for comparison with observational data. Whereas such comparisons do not strictly validate the derivation, since the probabilistic curves represent a class of structure not a single bridge, they lend some credence to the derived formulation. Valuable empirically-calculated vulnerability curves were obtained by Basöz *et al.* (1999) and Yamazaki *et al.* (1999). The former utilised a dataset compiled for the 1994 Northridge earthquake, whilst the latter employed data from the 1995 Hyogo-ken Nanbu (Kobe) earthquake of 1995.

In the current work methods based on vulnerability curves are adopted to assess the seismic behaviour of existing bridges. The advantages of employing vulnerability curves and DPMs is that the effect of the behaviour of structural components and material properties on the vulnerability can be better interpreted than with other statistical methods. Furthermore, uncertainties emanating from engineering judgment just affect the definition of damage level. They might, therefore, be reduced since the choice of limit states that quantify the level of damage may be verified by comparison with observations and experimental results on an individual structure basis.

1.4 Characterisation of ground motion and structural damage

A brief review of the available options for characterising structural damage and the severity of input motion is presented in the following. This is not intended as a review of the available literature, but rather an overview of the available options leading to the selection of hazard characterisation for the current study.

1.4.1 Ground motion

It is difficult to determine a single parameter that best characterises earthquake ground motion. Recorded time-histories, even at the same site, show variations in details. Earthquake ground motion amplitude, frequency content, duration and the number of peaks (and even their sequence) in the time-history above a certain amplitude are some of the important characteristics that affect structural response and damage. The frequency content of an earthquake time-history is important for the identification of the amount of energy imparted at different frequencies. Numerous parameters have been used to relate ground motion to the degree of damage sustained by a structure. Perhaps the most commonly used parameter is peak ground acceleration (PGA), and more recently spectral acceleration and displacement. Nevertheless, many other parameters, such as Housner spectral intensity, Arias intensity, root mean square acceleration and perceived intensity (e.g. MMI, MSK, MCS, JMA etc) may be employed to describe the input motion severity.

1.4.2 Structural damage

During strong earthquakes the cumulative damage caused by repeated load reversals degrades the resistance of structures. In order to quantify the cumulative damage of structures, damage indices have been introduced, the classification of which may depend on:

- displacement quantities;
- hysteretic dissipated energy;
- stiffness degradation;

When indices based on displacement or stiffness degradation are used, only the cycle with the maximum amplitude is considered. Other cycles are simply neglected. On the other hand, considering hysteretic energy as the damage parameter and assuming that collapse occurs when the structure dissipates an amount of energy equal to the limiting value, the contribute of all cycles is accounted for. Therefore, indices considering both displacement quantities and energy dissipation seem to be the most appropriate for describing the level of damage sustained by structures. However, the parameters that combine the damage due to excessive deformation and dissipated energy have a large variability, rendering recommending definitive values rather difficult.

Notwithstanding its limitations, PGA was selected to characterise earthquake intensity in this study, whilst structural limit states are described in terms of displacements. The former choice is a consequence of how the observational data used, to lend weight to the derivation, is expressed. The latter decision is a consequence of the increasing significance of deformation-based assessment and design approaches within a framework of performance targets for structural systems.

2. Derivation of empirical vulnerability curves

2.1 Approach used

Hereafter, observational vulnerability curves are reviewed and homogenised. Two data sets are employed. Caltrans compiled a data set for bridge damage during the 1994 Northridge earthquake whilst the Japan Highway Public Corporation (JH) gathered data for the 1995 Hyogo-ken Nanbu (Kobe) earthquake. This information was employed in previous work to obtain vulnerability curves for the Northridge and Kobe earthquakes independently (Basöz and Kiremidjian 1997, Yamazaki *et al.* 1999). In order to describe the damage condition of bridges, 5 'states' were considered: no damage, minor damage, moderate damage, major damage and collapse.

No subdivision of the bridges into different structural forms is attempted, due to lack of a viable sample per structural form. The vulnerability functions are meant to be average values for populations of bridges. However, it is obvious that vulnerability curves depend on the seismic code and the structural type of bridges used. A further classification based on other structural parameters, such as number of spans, abutment type, column bent type and span continuity was also employed. However, due to lack of data, important parameters in terms of bridge vulnerability such as previous reconstruction history or upgrading, seat width and column height were not included.

2.2 Damage probability matrices of the 1994 Northridge earthquake

Basöz and Kiremidjian (1997) and Basöz *et al.* (1999) utilised a data set compiled for the 1994 Northridge earthquake to obtain vulnerability curves for most significant structural types of bridges. The data set gives four sets of data:

- structural characteristics;
- bridge damage;
- repair costs;
- ground motion levels.

Bridge inventory data contains information on the physical characteristics of bridges in Los Angeles, Ventura, Riverside and Orange Counties. Structural characteristics include abutment type, number of

spans, type of superstructure and substructure, length and width of the bridge, skewness, number of hinges at joints and bents, abutment and column foundation types and design year to represent design standards. The data set was extracted from the Caltrans Bridge Maintenance Database (Caltrans 1993). The assumed ground motion parameter is the peak ground acceleration (PGA).

Table 1 Damage matrix for all highway concrete bridges in Greater Los Angeles area (Basöz and Kiremidjian 1997)

Observed Damage	Peak Ground Acceleration (g)										Total
	0.15-0.2	0.2-0.3	0.3-0.4	0.4-0.5	0.5-0.6	0.6-0.7	0.7-0.8	0.8-0.9	0.9-1.0	>1.0	
None	318	502	234	50	34	29	24	29	16	16	1252
Minor	2	10	25	2	6	4	6	1	7	3	66
Moderate	1	15	13	11	10	9	5	4	9	4	81
Major	0	10	2	6	7	3	2	5	11	1	47
Collapse	0	0	1	0	0	0	0	2	2	1	6

In Table 1 the number of bridges belonging to each level of damage at different PGA values for highway bridges in the Greater Los Angeles, from the work of Basöz and Kiremidjian, area are reported.

2.3 Damage probability matrices of the 1995 Hyogo-ken Nanbu (Kobe) earthquake

Japan Highway Public Corporation (JH) is in charge of the 6400 km long highway network. JH deployed a network of 123 accelerometers (1 instrument per 40 km) before the Kobe earthquake. A further 202 instruments were deployed after the earthquake. Yamazaki *et al.* (1999) collected damage data for the JH structures after the Kobe earthquake. As in Basöz *et al.* (1999) the objective of this investigation was to define a relationship between earthquake damage to highway structures and input motion intensity.

In the work of Yamazaki *et al.* (1999) a method for estimating the spatial distribution of earthquake ground motion was proposed. The Kriging technique, a method of stochastic interpolation, is employed to estimate ground motion indices from recorded values. Since the earthquake motion at the ground surface is affected by amplification characteristics of the surface layers, an amplification ratio was also evaluated. The parameters considered representative of the ground motion were PGA, PGV and JMA intensity.

Table 2 Damage matrix for all the JH concrete bridges (Yamazaki *et al.* 1999)

Observed Damage	Peak Ground Acceleration (g)										Total
	0.15-0.2	0.2-0.3	0.3-0.4	0.4-0.5	0.5-0.6	0.6-0.7	0.7-0.8	0.8-0.9	0.9-1.0	>1.0	
None	80	34	23	28	12	3	3	1	0	0	184
Minor	0	0	2	1	0	4	0	1	0	0	8
Moderate	0	0	1	3	3	6	0	0	0	0	13
Major	0	0	0	1	0	5	1	0	0	0	7
Collapse	0	0	0	2	0	2	0	0	0	0	4

In the 1995 Kobe earthquake heavy damage was inflicted on highway structures. In the data set of Yamazaki *et al.* (1999), 216 bridges on 4 routes were investigated. The DPM employed in the latter study is shown in Table 2.

2.4 Vulnerability curves for reinforced concrete bridges based on observational data

The DPMs reported in Tables 1 and 2 are herein used to derive vulnerability curves based on observational data, in order that the procedure used herein is verified versus the work reported in the above two references. Moreover, a set of curves using the combined USA and Japan data is sought. Table 3 summarises the size of the sample for all the assumed damage states.

Table 3 Sample size for the assumed damage levels

Observed Damage	Sample Size
None	1436
Minor	74
Moderate	94
Major	54
Collapse	10

The vulnerability curves must be representative of the cumulative probability of occurrence of damage equal to, or higher than, a certain level. Therefore, the first step of this analysis is the determination of an appropriate statistical distribution. Towards this end, the histograms of the sample distribution were plotted as shown in Fig. 2 and examined for trends.

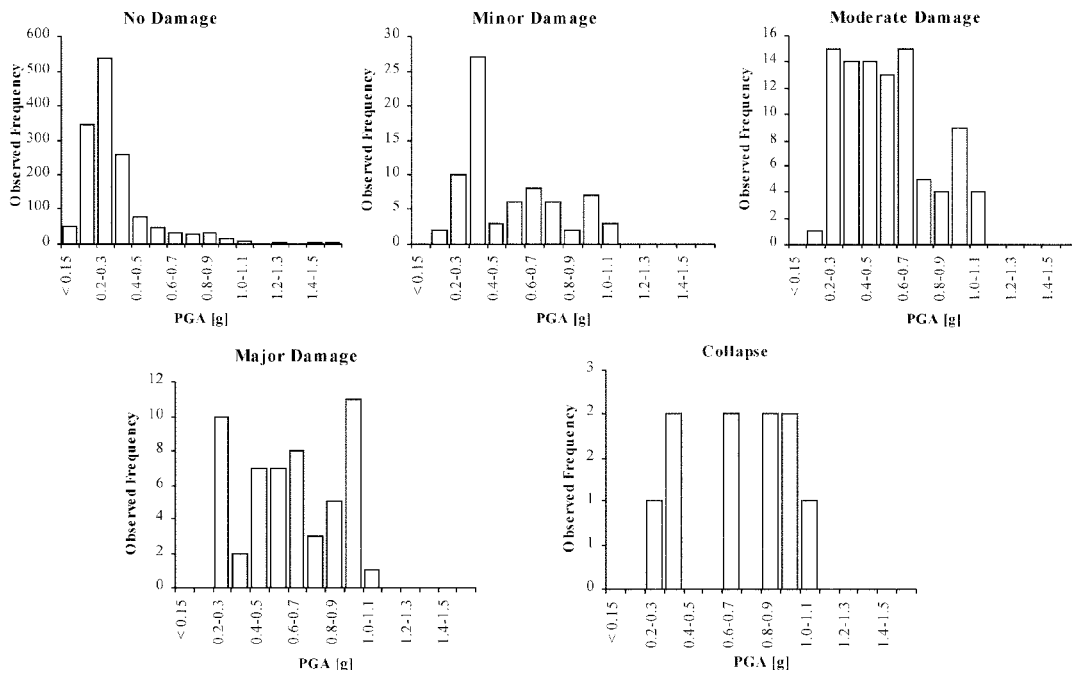


Fig. 2 Observed distribution of the sample for all the considered damage levels

This indicates that both normal and lognormal distributions are suitable models for the sample under consideration. It is shown, however, that an asymmetric distribution is more appropriate to represent the low damage states, whilst the distribution of the sample is almost symmetric for high damage levels. Therefore, the cumulative probabilities may be given by either of the following:

$$P_R(\text{PGA}) = \Phi((\ln \text{PGA} - \lambda)/\xi) \quad (1)$$

$$P_R(\text{PGA}) = \Phi((\text{PGA} - \mu)/\sigma) \quad (2)$$

where Φ is the standard normal distribution, λ and ξ are the mean and standard deviation of $\ln(\text{PGA})$ and μ and σ are the mean and standard deviation of PGA. The parameters in the Eqs. (1) and (2) were estimated using the sample data and are reported in Table 4 for PGA in g.

Table 4 Parameters for the normal and lognormal distributions

Observed Damage	Normal Distribution		Lognormal Distribution	
	μ	σ	λ	ξ
None	0.315	0.193	-1.315	0.566
Minor	0.516	0.249	-0.766	0.458
Moderate	0.554	0.239	-0.677	0.414
Major	0.618	0.255	-0.561	0.397
Collapse	0.733	0.239	-0.362	0.318

The Kolmogorov-Smirnov test (K-S test) is used to assess the quality of the statistical fit. The procedure involves comparison between the experimental cumulative frequency and the assumed theoretical distribution functions. The maximum difference D_{MAX} between the theoretical distribution and the observed cumulative distribution is taken as a measure of viability. Fig. 3 shows the considered theoretical distributions (for lognormal and normal models) and the cumulative distribution directly evaluated by the sample for each damage level. The values of D_{MAX} calculated for all damage levels are reported in Table 5.

Table 5 D_{MAX} from the K-S test

Observed Damage	Lognormal Distribution	Normal Distribution
None	18.2	26.4
Minor	23.2	24.7
Moderate	12.7	11.7
Major	16.6	11.0
Collapse	18.8	16.1

The K-S test confirms the observation from the frequency distribution of the sample (Fig. 2). For low levels of damage the lognormal model fits better the observed distribution, whilst the normal

distribution is a more suitable model for high level of damage. In the current study the lognormal distribution is assumed to represent vulnerability curves for all the damage conditions. This choice is supported by the following considerations:

- The collapse limit state, and in its vicinity, is unlikely to occur for bridges designed to modern seismic codes, such as the bridges studied analytically hereafter.

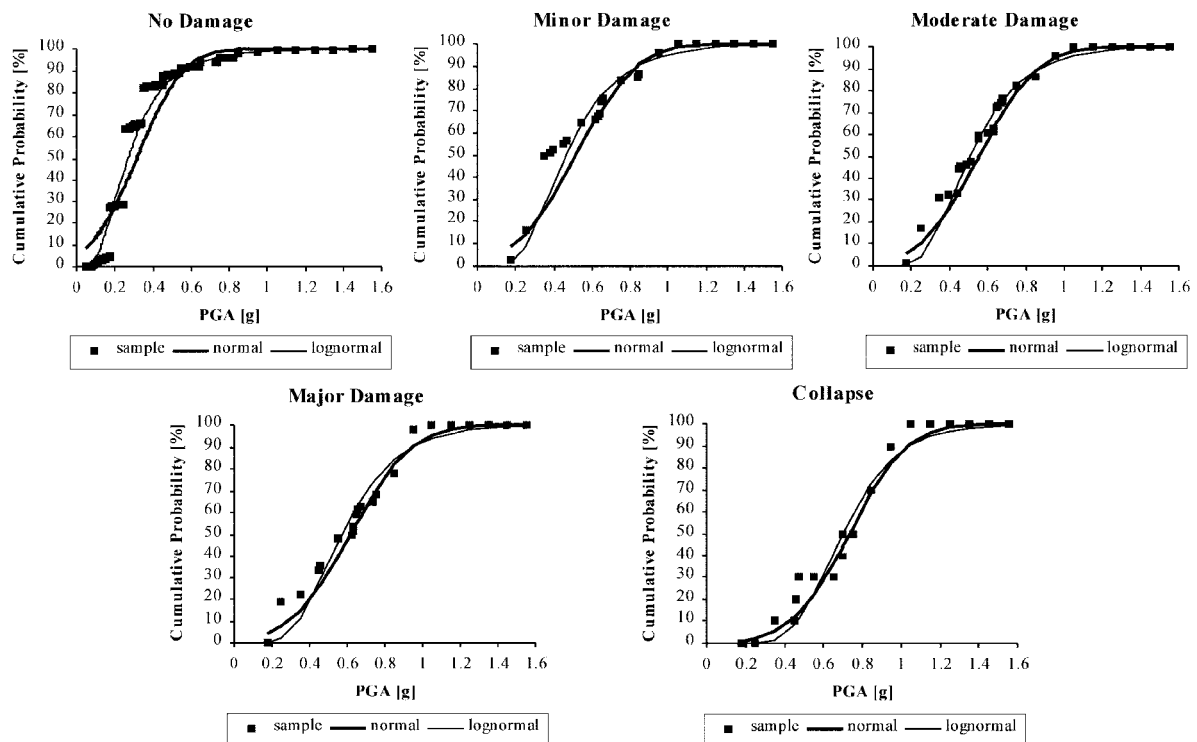


Fig. 3 Comparison between the observed cumulative distribution and normal and lognormal distributions

- Medium-near or large-distant earthquakes are more frequent than large-near events; hence the probability of sustaining low-to-medium damage is higher than otherwise.
- The statistical viability of the sample used is more convincing for the low-to-medium damage states.

The assumption made is therefore considered appropriate for the description of damage levels for a large population of reinforced concrete bridges.

In Fig. 4 the vulnerability curves for Northridge, Kobe and their combination are shown. The Kobe results are less smooth than for Northridge. This is attributable to the sparseness of the data (Table 2.2). It may therefore be that the Hyogo-ken Nanbu data are statistically non-viable if viewed in isolation. It is, however, a useful addition and verification of the available Northridge data.

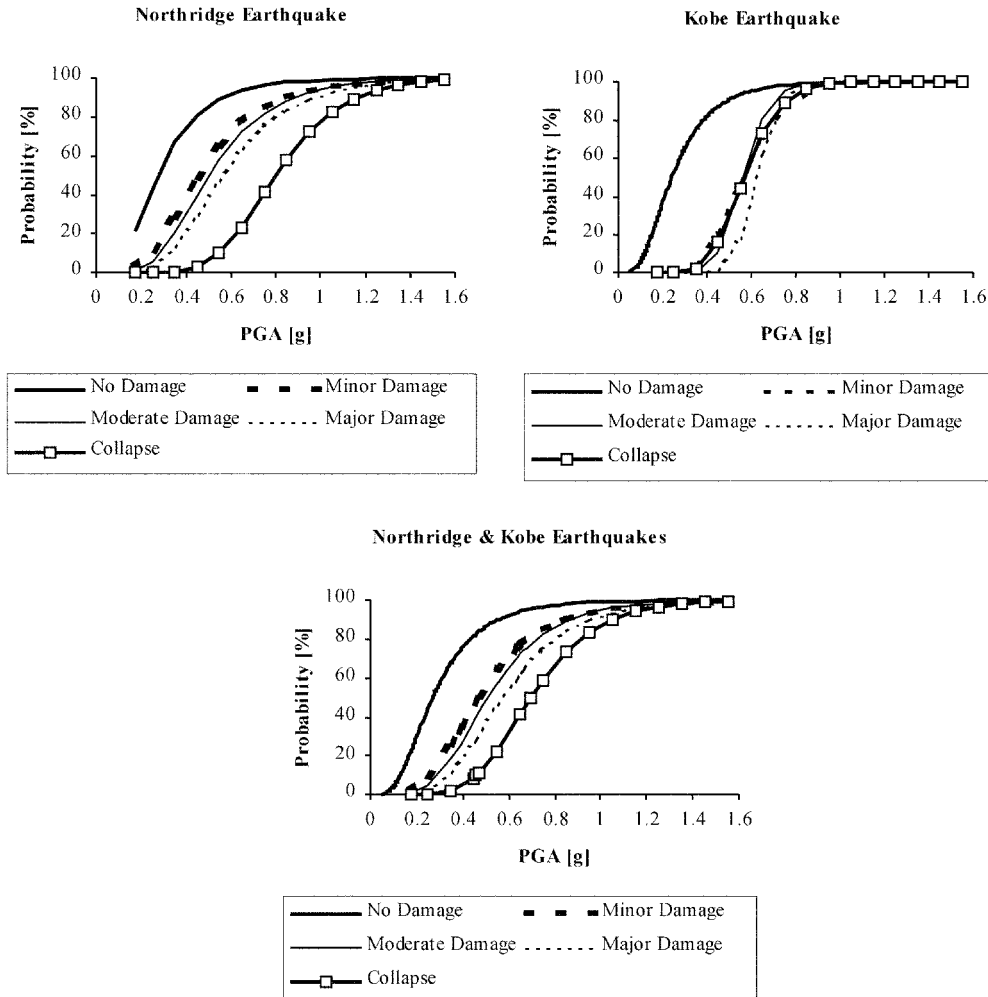


Fig. 4 Vulnerability curves for the two events considered

2.5 Remarks

Consistent, viable and evenly distributed (spatially and limit-state-wise) data for seismic damage of bridges are unavailable; a situation that is observed, to a lesser extent, for buildings (Rossetto and Elnashai 2003). However, it is likely that the quality of data points for bridges (the consistency and reliability of field-collected data) is higher than for buildings, as a consequence of the smaller number of damaged structures and also the training of engineers undertaking damage surveys. Above, the best available (published) data was employed to explore the feasibility of deriving vulnerability functions. Emphasis was placed on low and medium damage levels; therefore the statistical model that fits best the data in this range was employed. The derived curves exhibit the shape and features expected, in qualitative comparisons with building vulnerability functions. Their reliability as a predictive tool, though, requires further work. One option is to enrich the observational functions with analytical investigations. This option is pursued further hereafter.

3. Analytically-derived vulnerability functions

Based on deformational quantities, a procedure is outlined herein to enrich observational vulnerability curves with analytical counterparts and provide both approaches with a degree of mutual verification if the results are not vastly different. Typical material variability values are determined with the aim of describing deformational quantities that represent different limit states. Subsequently, vulnerability curves for a particular bridge are determined using the proposed procedure. These curves are compared to the observational functions derived in previous sections of this paper. Finally vulnerability curves for three different configurations (variations of the first model) are compared and the possibility of parametrically-described curves is explored. The latter work is undertaken to explore the feasibility of deriving vulnerability curves that represent not just the bridge investigated but a wider variety of bridges of the same type, thus reducing or eliminating the required extensive analytical effort. It should be emphasised at the outset that close agreement between the observational curves and their analytical counterparts is not, strictly, a verification of the latter, which are derived using detailed section-level limit states of a specific bridge. This is discussed further in subsequent sections.

3.1 Description of the procedure

The proposed procedure for the definition of vulnerability curves uses a displacement-based approach to define the damage inflicted on the bridge. Therefore, the probability of reaching or exceeding a damage state is derived by comparing the displacement response of the bridge and the displacement demand corresponding to certain input motion intensity, described in terms of PGA. The procedure requires the use of a verified inelastic dynamic analysis tool. Consideration has been given to the use of an inelastic static procedure, such as Capacity Spectrum Method. However, in the work of Shinozuka *et al.* (2000), it was reported that the latter approach matches well fragility curves derived by inelastic dynamic analysis only for low damage limit states. At higher damage levels and limit states approaching collapse, the static and dynamic methods diverge. It was therefore decided to employ inelastic dynamic analysis.

The uncertainties associated with the displacement capacity of the bridge are accounted for by assuming variable material properties. According to common seismic design practices, the structural elements in which damage is concentrated are the bridge piers. Therefore, to evaluate the displacement capacity corresponding to different damage levels, pushover analysis of the bridge piers is employed. A sample of randomly generated material properties is used in the pushover analyses as subsequently discussed in detail. The outcome of the analyses is the distribution of displacement capacity of the bridge piers.

To evaluate the displacement demand, inelastic dynamic analyses are required. The PGA levels assumed in the definition of the vulnerability curves are used to scale the accelerograms employed as input motion in the aforementioned analyses. The displacement demand is represented by the peak transient displacement recorded at the top of the piers. In this step of the procedure the average values of material properties are employed. The outcome of these analyses is the distribution of probability of the displacement demand. Thereafter, a code spectrum-compatible artificial accelerogram is employed as input motion for the whole range of PGA by successively scaling its PGA. The assumption employed in so doing is that for all the considered PGA values the displacement demand follows the same distribution determined for the selected single value of

PGA. This assumption could be abandoned in future studies and the set of accelerograms used in the whole range of limit states. For the current study, the level of detail in the structural model is given priority.

The probability of reaching a certain limit state (P_{LSi}) is given by:

$$P_{LSi} = \int_0^{\infty} f_C(\Delta)(1 - F_D(\Delta))d\Delta = \int_0^{\infty} f_D(\Delta)F_C(\Delta)d\Delta \quad (3)$$

where f_C and F_C are the probability density functions and the cumulative probability of the displacement capacity, F_D is the cumulative probability of displacement demand and Δ is the random variable. In this procedure Δ corresponds to a displacement.

3.2 Limit states definition

Five post-earthquake damage states are employed. These are as follows:

- Undamaged;
- Slightly damaged, but usable without repair or strengthening;
- Extensively damaged, but still repairable
- No collapse, but so severely damaged that must be demolished;
- Collapse.

To assess these five possibilities four limit states have to be defined. In the case of bridges design to modern seismic codes, it is not necessary to distinguish between the latter two states of the list above, since collapse should not occur. Therefore, the classes can be reduced to four. On the basis of experimental results reported in the technical literature the limit states are defined as follows:

- LS1 Below this LS no damage should take place and the expected response is of small displacement amplitude. To define the position of the yield point on the force-displacement curve of the piers the proposals of Park and Pauley (1975) and Pauley and Priestley (1992) are invoked. These depict that yielding of the first longitudinal row of reinforcing bars occurs at a level of transverse load equal to 75% of the yield load V_y .
- LS2 Below this LS only minor structural damage should be observed and the bridge is usable after the earthquake. Member flexural strengths may have been reached, and limited ductility developed, provided that concrete spalling in plastic hinges does not occur and that residual crack widths remain sufficiently small. The deformation of the cover concrete ϵ_c is assessed to identify this limit state. It is compared with the ultimate compression deformation capacity of unconfined concrete. US practice (ACI 318) recommends a maximum usable strain of 0.3%, but at this strain level, the compressed concrete in a flexural member will not normally show crushing or spalling. Experimental results reported by Mattok *et al.* (1961) indicate that the limit of deformation of unconfined concrete is variable, therefore the experimental results of Hognestad (1951) are used. In the latter work tests of 120 reinforced concrete columns are reported, 90 of which are of square and 30 of circular cross-section. The average values and the COVs calculated considering individual groups and all the groups together are reported in Table 6.

Table 6 Average and COVs values of ε_c (Hognestad 1951)

Group	Average	COV
Group I	3.71‰	15.16%
Group II	4.22‰	17.17%
Group III	3.88‰	10.23%
Group IV	3.20‰	19.31%
Total	3.65‰	19.10%

- LS3 Below this LS significant structural damage is expected. The bridge will be out of service after the earthquake unless significant repair is undertaken. However, repair and strengthening is feasible. Rupture of transverse reinforcement or buckling of longitudinal reinforcement should not occur and core concrete in plastic hinge regions should not need replacement. Experimental results that enable the evaluation of the limiting deformation in the concrete or steel representative of this damage state are not available. Therefore, a displacement capacity that is the average of LS2 and LS4 is herein assumed pending further refinement, as information becomes available.
- LS4 Below this LS extensive damage is expected, but the bridge should not have collapsed. Repair may be neither possible nor cost-effective. The structure will have to be demolished after the earthquake. Beyond this LS global collapse endangering life is expected since it corresponds to the inability of the structure to sustain gravity loads. The results of experimental tests undertaken by Hoshikuma *et al.* (1997) on bridge piers with circular, square and wall sections showed that crushing of confined concrete and buckling of longitudinal reinforcement occurs when the compression stress drops to less than $0.5 f'_{cc}$. Because such damage is excessive and irreparable, the strain corresponding to $50\% f'_{cc}$ is assumed as the ultimate strain ε_{cu} . A random variable X , that represents the ratio of analytical and experimental values of ε_{cu} , is assumed to account for the uncertainty in terms of confinement. The statistics of this random variable were obtained by Kappos *et al.* (1998) for the Kent and Park empirical confinement model. The collapse criterion considered in the latter work is that proposed by Park and Pauley (1975) in which ε_{cu} corresponds to a residual stress of 85% of the unconfined resistance f_c . However, the statistics of X are applicable to other criteria, since the post-peak branch of the stress-strain curve of concrete is not far from linearity, as confirmed by experimental results. The average value and the COV of X are reported in Table 7.

Table 7 Statistics of the ratio experimental-to-analytical values of ε_{cu} for the Kent and Park confinement model

X_m	COV
1.140	38.5%

The deformation of steel is also investigated for this limit state. From the values proposed by Pipa and Carvalho (1995) a strain of 9% is assumed. No further refinement is warranted, because the deformational capacity of the steel is very rarely exceeded before other limit states are satisfied.

3.3 Application example

The procedure outlined above is intuitive and reflects the current state-of-art in vulnerability functions. Several assumptions were made that were based on observational data. Herein, an example application is undertaken to gain insight into the proposed analytical procedure. The bridge analysed is straight 60 metres long and 16 metres wide and is part of the Egnatia Othos road network currently under construction in northern Greece. A similar treatment applies to skew bridges, if use is made of simplified procedures to represent such bridges (e.g. Ming *et al.* 2001). The superstructure is supported by the abutments and by two rows of piers. The superstructure is a hollow prestressed concrete deck, while the piers comprise three reinforced concrete circular columns directly connected to the deck, which is connected to the abutments by elastic bearings. The characteristics of the concrete and reinforcement of the piers are B25 and S500, respectively. The bridge model considered is shown in Fig. 5.

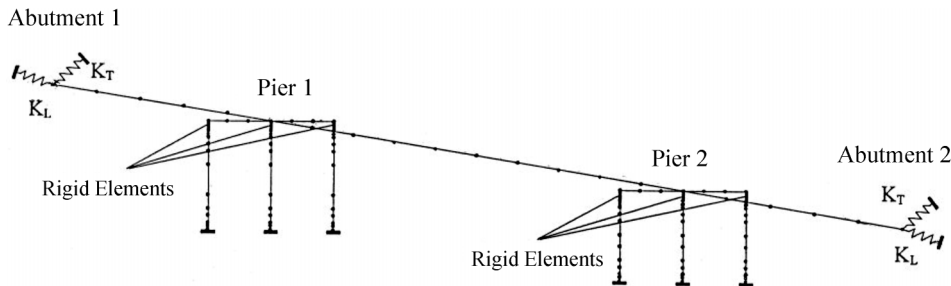


Fig. 5 Finite element model of Bridge 1

The finite element package employed to analyse the bridge is ADAPTIC. This program is specific to the inelastic large displacement analysis of frames and was mainly developed by Izzuddin and Elnashai (1991) with contributions from many other researchers from Imperial College, London, UK.

3.4 Modelling of material variability

3.4.1 Steel model

The behaviour of the reinforcement is represented by means of the bilinear elasto-plastic model with kinematic hardening. The parameters of this model are the yield stress f_y , Young's modulus E and the post-elastic stiffness coefficient α . Based on previous studies on effect of random variability of steel materials on seismic response (Elnashai and Chryssanthopoulos 1991), the random variable used for reinforcing bars is the yield stress of the reinforcement f_y . The results of an investigation of the characteristics of steel reinforcing bars were presented in Pipa and Carvalho (1995), where a normal distribution of steel resistance was assumed. The coefficient of variation (COV) proposed in the latter study for B500 steel is adopted. The characteristic value represents the resistance below which 5% of the sample falls. Therefore, knowing the COV and the 95% fractile values, the nominal value of resistance, which corresponds to the average value of the distribution, is calculated. The parameters of the distribution, including characteristic, average and COV values are reported in Table 8.

Table 8 Statistics of the steel yield stress

f_{yk}	f_{yn}	COV
500 MPa	550 MPa	5.2%

Young's modulus E is assumed as deterministic and equal to 200 kN/mm² (EC2), because low levels of variability of this parameter have been observed. As a consequence of the high deformation capacity of steel and the limit imposed by modern seismic design codes on the ratio between the ultimate stress (f_u) and the yield stress (f_y), the coefficient α , representing strain-hardening, which accounts for the post-elastic stiffness, is rather low. Therefore, it is not significant to take into account the variability of this parameter. A deterministic value of α equal to 0.5% is proposed for the analyses.

3.4.2 Concrete model

The stress-strain relationship for the concrete model implemented in ADAPTIC, was employed (Martinez-Rueda and Elnashai 1996). The parameters of the model are the concrete compressive strength (f'_c), the concrete tensile strength (f_t), the crushing strain ϵ_{c0} and a confinement factor. The compression resistance is the only random variable that is allocated a normal distribution in common with previous studies. Mirza *et al.* (1979) suggest COV values for the distribution of compressive resistance of cylinder specimens equal to 12%, 15% and 18% for precast, ready-mix and in-situ concrete, respectively. In this case, the COV value that represents the assumed construction of the bridge is 18%. The characteristic, average and COV values of the concrete compressive resistance are reported in Table 9.

Table 9 Statistics of the concrete compressive strength

f_{ck}	f'_c	COV
25 MPa	35 MPa	18%

The tensile resistance f_t of concrete is neglected, since it was observed that this parameter does not have a significant influence on the response of RC structures responding in flexure. Concrete stress-strain relationships obtained by tests on cylinders subjected to axial loads have shown that the peak stress approximately corresponds to a deformation of 0.2%, the value associated with the cracking deformation ϵ_{c0} .

3.5 Bridge model

In the finite element model of the bridge, the abutments and the deck are modelled using elastic elements while fibre elements that describe the behaviour of reinforced concrete members are used for the bridge piers. The piers are considered fully restrained at the base. Elastic spring elements are used to model the bearings and the expansion joints between the deck and abutments. The stiffness of the expansion joint K_L is assumed 5.43×10^6 kN/m. The spring that represents the connection between abutment and deck in the transverse direction has a stiffness K_T of 8×10^3 kN/m. This stiffness value corresponds to almost 5%Wmm⁻¹ (Ghobarah and Ali 1988) where W is the

superstructure weight on the abutment. The stiffness suggested by Ghobarah and Ali (1988) can be considered as a lower bound. An uncertainty on the stiffness of the bearings has to be taken into account. This is due to the fact that the behaviour of these devices is a function of the axial load as well as the relative displacement between abutment and deck. Those parameters are variable under earthquake loads. The uncertainty factor is assumed to be 2 (Priestley *et al.* 1996). Therefore K_L is assumed to be in the range of 8×10^3 to 16×10^3 kN/m.

Rigid elements are used to connect the top of the columns, in order to represent the large stiffness of the deck in the transverse direction and to locate the centre of masses on the deck axes in the dynamic analyses. The model is shown in Fig. 5.

3.6 Analysis of the bridge

3.6.1 Pushover analysis of the piers

To quantify the deformational supply (capacity) of the piers, static inelastic pushover analysis is employed. The load conditions are:

- vertical loads on the columns representing the dead and live loads;
- horizontal displacements normal to the deck axis.

In order to identify the displacement capacity corresponding to the selected limit states, the stress and deformations in the reinforcement, confined and unconfined concrete are monitored and mapped into the load-displacement curve.

To quantify the uncertainty in the displacement capacity of the system a sample of randomly-generated numbers was used for material properties. As a first trial a sample size of 30 values was used. This was contrasted with a sample of 40 random values. The average and COV of random variables was calculated to assess the viability of the sample, as reported in Table 10.

In Tables 11 and 12 the average and COV of the displacement capacity for the two sample sizes are reported. The average and standard deviation seem insensitive to the sample size, for the limited range considered. Therefore, further increase of the sample size is not necessary, at least in the vicinity of the two sizes tested in Tables 10, 11 and 12.

Table 10 Average and COV of the randomly generated samples

	f_y [kN/mm ²]		f'_c [kN/mm ²]		ϵ_c		X	
	Average	COV	Average	COV	Average	COV	Average	COV
30	547.8	5%	35.2	17%	3.60‰	19%	1.19	38%
40	548.0	5%	34.8	17%	3.68‰	19%	1.15	39%

Table 11 Average and COV values of the displacement capacity of pier 1

	Δ_{LS1} [mm]		Δ_{LS2} [mm]		Δ_{LS3} [mm]		Δ_{LS4} [mm]	
	Average	COV	Average	COV	Average	COV	Average	COV
30	47	6	64	11	103	18	142	25
40	47	5	65	11	103	17	142	24

Table 12 Average and COV values of the displacement capacity of pier 2

	Δ_{LS1} [mm]		Δ_{LS2} [mm]		Δ_{LS3} [mm]		Δ_{LS4} [mm]	
	Average	COV	Average	COV	Average	COV	Average	COV
30	34	6	47	11	78	18	110	26
40	34	6	47	11	78	18	109	25

A suitable model for the distribution of the displacement capacity is required. The normal and lognormal cumulative distributions are tested and the parameters of the idealised distribution are reported in Table 13. As in previous sections of this paper, the Kolmogorov-Smirnov test (K-S test) is used to study which of the candidate distributions fits better the calculated points. The maximum difference D_{MAX} between the theoretical distribution and the observed cumulative functions are reported in Table 14. For both piers at the limit states corresponding to a low level of damage, the normal distribution provides a better fit. On the other hand, the lognormal model fits better cases of high damage.

3.7 Dynamic analyses

Inelastic time-history analyses were undertaken to evaluate the displacement demand on the bridge piers using 7 accelerograms. Table 15 lists the characteristic of the earthquakes from which the natural strong-motion records were obtained. The number and specific records selected have a negligible effect on the vulnerability curves since they are used only to define a displacement demand distribution. They have been selected, however, to represent earthquakes with magnitudes below 7 and above 5.5, typical of areas of moderate seismic hazard, which constitute the majority of earthquake-prone areas in the world. Moreover, short-to-moderate epicentral distances from the source to the measuring station were chosen because at longer distances, such magnitude earthquakes produce low acceleration values that would have required substantial scaling. The accelerograms were scaled to the design value of PGA (0.2 g). The results were used to assess the uncertainty in displacement demand. A lognormal distribution is assumed to fit the results obtained with the aforementioned inelastic dynamic analyses. This is a decision taken, since the seven points obtained do not constitute a sample amenable to statistical representations. The parameters of the lognormal distribution are reported in Table 16.

Table 13 Parameters of the statistical distribution of displacement capacity

		Normal Distribution		Lognormal Distribution	
		μ	σ	λ	ξ
Pier 1	LS1	47.27	2.54	3.85	0.05
	LS2	64.76	7.04	4.16	0.11
	LS3	103.19	17.31	4.62	0.17
	LS4	141.63	34.34	4.92	0.24
Pier 2	LS1	34.26	1.94	3.53	0.06
	LS2	47.02	5.38	3.84	0.11
	LS3	78.06	13.75	4.34	0.17
	LS4	109.09	27.37	4.66	0.25

Table 14 K-S test for two statistical distribution model for displacement capacity

		D _{MAX} , Normal	D _{MAX} , Lognormal
Pier 1	LS1	25%	26%
	LS2	9%	11%
	LS3	13%	11%
	LS4	13%	11%
Pier 2	LS1	29%	30%
	LS2	10%	12%
	LS3	12%	9%
	LS4	14%	11%

Table 15 Characteristics of selected earthquakes

Earthquake	Date	Magnitude	Epicentral Distance
Erzincan, Turkey	13/03/1992	6.8	4 km
Friuli, Italy	11/09/1976	5.5	7 km
Patras, Greece	14/06/1993	5.6	8 km
Aegion, Greece	18/11/1992	5.7	25 km
Thessaloniki, Greece	20/06/1978	6.4	33.8 km
Kalamata, Greece	13/09/1986	5.8	12.8 km

Table 16 Parameters of the idealized distribution of displacement demand

	Lognormal Distribution	
	λ	ξ
Pier 1	3.37	0.40
Pier 2	3.12	0.38

The average values of material properties and stiffness of the bearings are used in the dynamic analyses. This assumption has been verified by comparing the response of the bridge for mean, mean $\pm\sigma$ and the upper/lower bound values. For this comparison a synthetic accelerogram generated to fit the Eurocode 8 spectrum, as a representative of modern seismic codes, was used, scaled to a PGA value of 0.4 g. This choice is based on the fact that the selected value of PGA should produce yielding in the bridge piers, otherwise the limiting resistance of materials is not exceeded and it is not possible to check their influence on the displacement demand. The results of this analysis show that the influence of the variability of material properties on seismic demand can be neglected and the recorded maximum displacements are given in Table 17. The influence of material resistance and stiffness of bearings is appreciable. However, those parameters seem to give an uncertainty in terms of displacement requirements that can be neglected compared to the influence of input motion.

Finally, displacement demand from inelastic dynamic analyses using the generated accelerogram is reported in Fig. 7, as a function of the PGA level for both bridge piers.

Table 17 Maximum displacement for different values of material resistance and bearing stiffness

	Mean	Mean +1 σ	Mean -1 σ
Pier 1	93.93 mm	98.78 mm	86.40 mm
Pier 2	48.27 mm	56.56 mm	58.44 mm

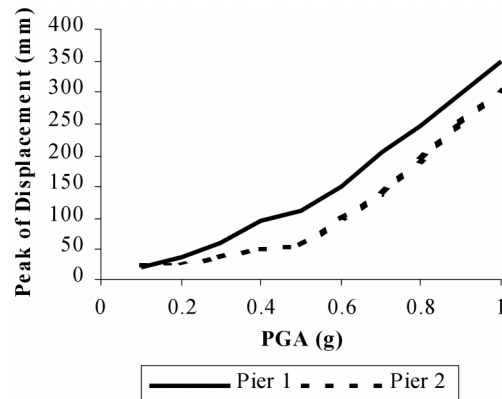


Fig. 6 Peak recorded displacements at the top of the bridge piers for code-compatible synthetic accelerogram

It is noteworthy that in general using many more records in the dynamic analysis is preferable. However, this would increase very substantially the analysis effort without a definable improvement in results. The true variability, in a probabilistic sense, comes into the application of vulnerability analysis through using probabilistically-based seismic demand quantities (e.g. intensity, PGA or other outputs of probabilistic seismic hazard analyses). Such an issue requires more extensive studies and is not discussed further herein.

3.8 Vulnerability curves

The bridge vulnerability curves were obtained assuming that a certain limit state is reached when one of the two piers attains that limit state, which is a conservative assumption. The vulnerability curves obtained are reported in Fig. 8, for the two piers and the entire bridge. The irregular shape of the vulnerability curves of pier 2 is due to the deformed shape of the first vibration mode. The average values and the standard deviations obtained on the basis of the obtained cumulative distributions are reported in Table 18.

Table 18 Average and standard deviation values corresponding to the evaluated cumulative distribution

Limit State	Average	Standard Deviation
1	0.355 g	0.154 g
2	0.429 g	0.165 g
3	0.563 g	0.178 g
4	0.666 g	0.180 g

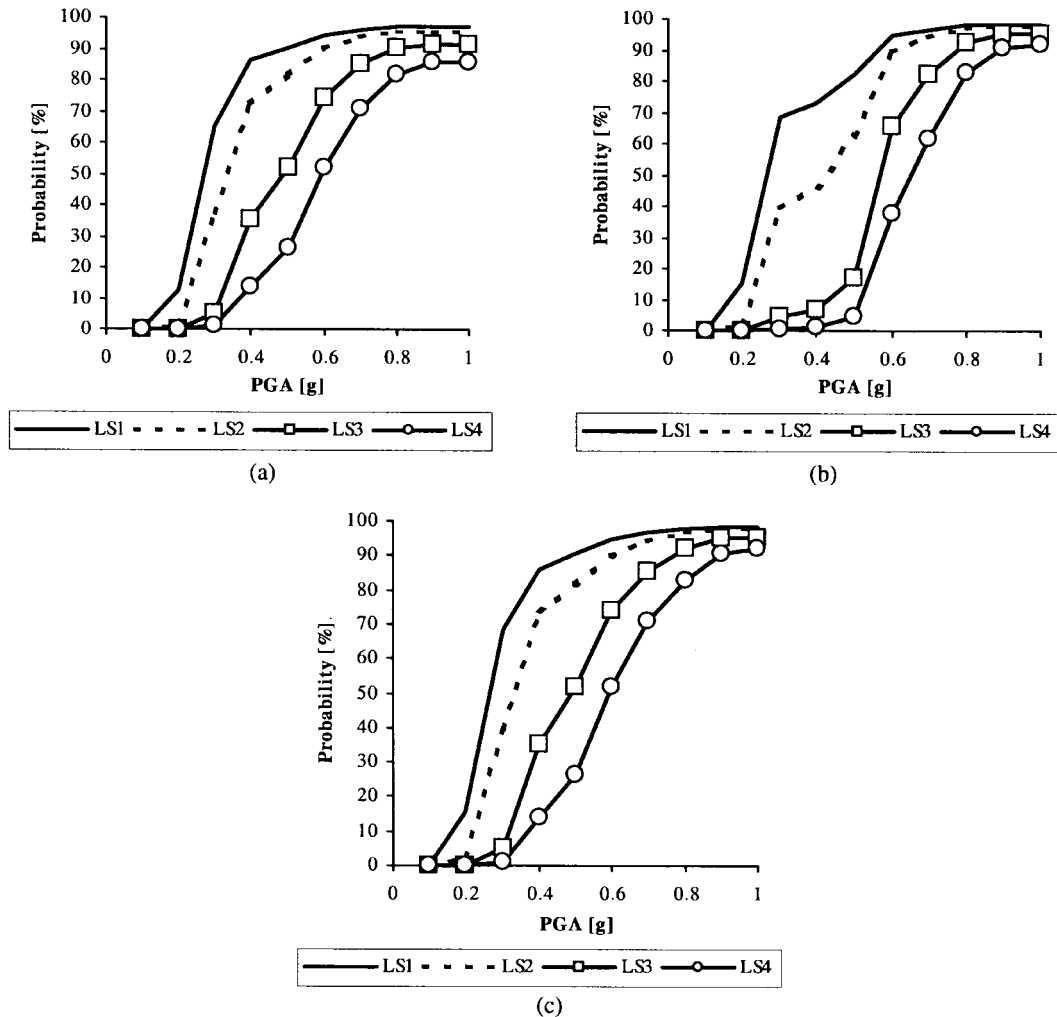


Fig. 7 Vulnerability curves for the (a) pier 1, (b) pier 2 and (c) bridge

The vulnerability curves calculated for the bridge were compared with the empirical functions derived in the first part of this paper, obtained from damage observations in previous earthquakes. These were classified for the damage states: none, minor, moderate, major and collapse. The empirical and calculated vulnerability curves are compared as indicated below:

- no damage with limit state 1;
- minor damage with limit state 2;
- moderate damage with limit state 3;
- major damage with limit state 4;

The calculated and empirical vulnerability curves are reported in Fig. 9 for the damage levels employed. The comparison is satisfactory for limit states 1, 3 and 4, whilst for limit state 2 large differences are observed. This is due to limit state 2 corresponding to the spread of cracks in only one of the structural elements of the bridge, an assumption leaning towards the over-conservative.

Globally, however, the level of agreement between observational and analytical vulnerability functions is reassuring. It is emphasized that this is not a formal validation of analytical curves, the validation of which can only be undertaken by comparison to large databases of damage to RC bridges similar to the above-described prototype bridge. The analytical functions derive their plausibility from the sound basis for their derivation, the rigour of the analytical models used and the general acceptability of their shape and the damage levels they predict.

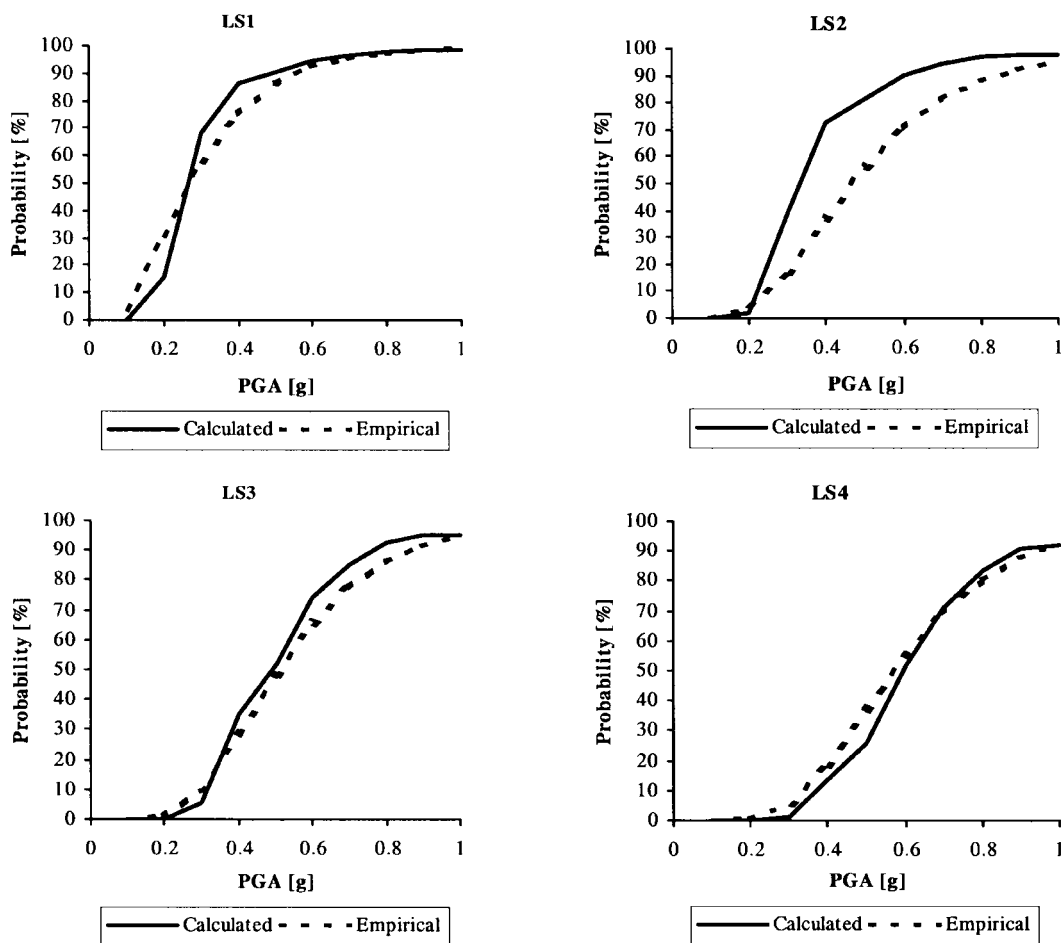


Fig. 8 Comparison between calculated and empirical vulnerability curves

4. Generalization of analytical functions

The curves derived above pertain to a specific bridge with fixed dimensions (i.e. pier and deck dimensions, span length etc). In principle, to investigate damage distribution in a region where similar but not identical bridges exist would require repeating the analytical study described above, using identical assumptions in order that the level of uncertainty in the results is maintained.

Hereafter an attempt is made to short-circuit the intensive analytical work required to derive vulnerability functions for bridges that are similar but not identical to the structure used as the basis of the example application above.

4.1 Geometric parameters influencing seismic response

Two parameters were selected for analysis aimed at generalizing the vulnerability functions, namely the diameter of the columns cross-section and the length of the spans of the bridge. The first (pier diameter) directly influences the capacity of the bridge as a whole, while the second (span length) causes an increase in design base shear. Both parameters will have a direct bearing on the overstrength (ratio of available-to-design base shear) of the bridge. This particular approach derives its validity from the correlation between level of observed damage and code base shear for the Hyogoken Nanbu, Japan, earthquake of 17 January 1995, as described by Kawashima and Onjoh (1996).

Three bridge configurations ensued. The first configuration has a reduced diameter of columns by 13%, in comparison with the first bridge, and is referred to as Bridge 2. A further decrease of 15% and an increase of 10% of the spans were applied for the second configuration, Bridge 3. The third configuration, Bridge 4, has the same columns diameter as Bridge 2 but has a 30% increase in span. The model characteristics are given in Table 19. Both the volumetric ratio of longitudinal reinforcement and the mechanical ratio of transverse reinforcement were kept constant. Consequently, the behaviour (or response modification) factor, referred to as R in US practice and q in European practice, is expected to remain constant. This is verified by the results of the pushover analyses where the behaviour factor, R or q , for the four bridges is around 3.

The geometry and overstrength parameters for the four bridges are given in Table 19, calculated from the peak of the pushover curve and the design base shear.

Table 19 Structural and geometric characteristics of studied bridges

	Bridge 1	Bridge 2	Bridge 3	Bridge 4
Pier Diameter (m)	1.5	1.3	1.3	1.1
Central Span (m)	30.5	30.5	39.65	33.55
External Span (m)	16.25	16.25	21.15	18.15
Behaviour Factor	3.2	2.9	2.7	2.9
Overstrength ratio	4	2.6	1.7	2.2

The same procedure for vulnerability curve definition as described above is applied for each bridge. The ensuing vulnerability curves are illustrated and compared in Fig. 9.

It is confirmed from Fig. 9 that the overstrength ratio is an appropriate parameter to use for distinguishing bridges that belong to the same class. From the four vulnerability curves examined in this study two pairs have almost identical shape. The curves of the two bridges with the higher overstrength ratio and the two with the lower overstrength ratio have almost identical shape but different values. Parameterizing the vulnerability curves by use of the overstrength ratio (ratio of available-to-required base shear) is therefore undertaken to derive simple expressions for deriving new curves once the overstrength ratio is defined from pushover analysis.

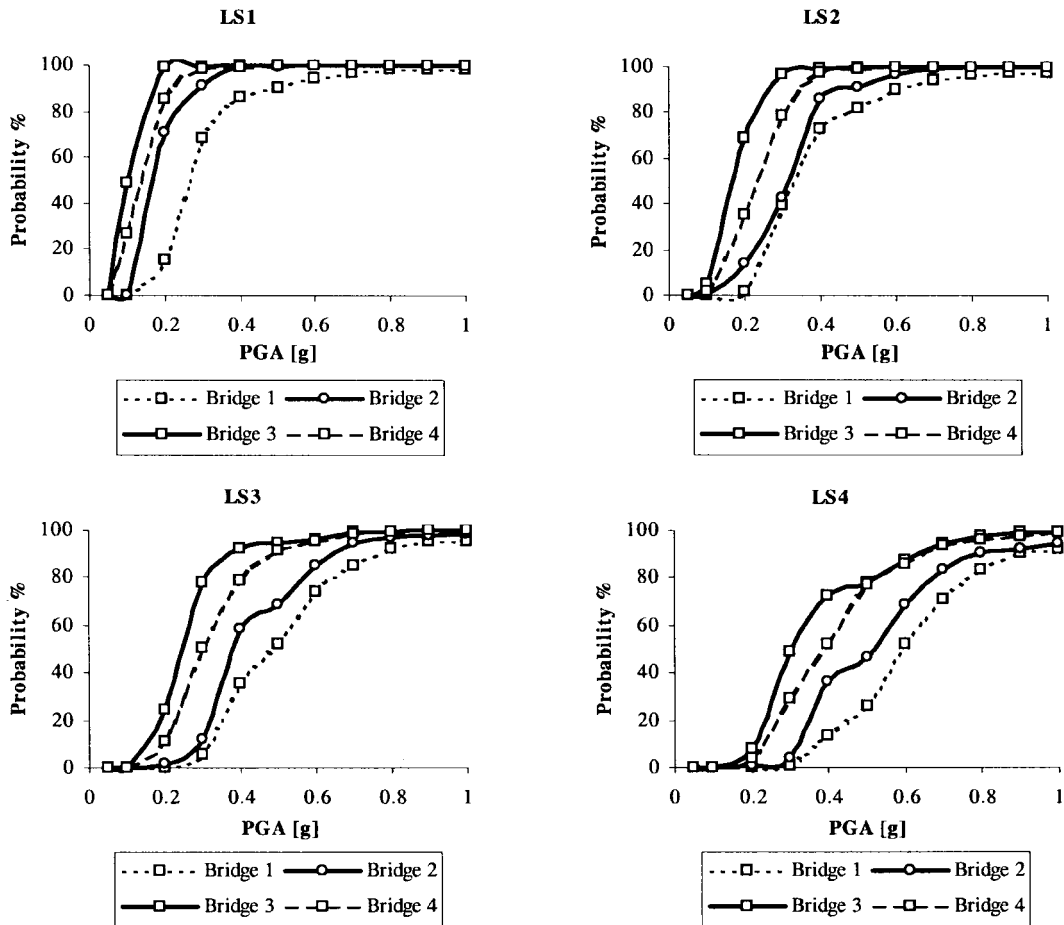


Fig. 9 Comparison of vulnerability curves of all the configurations for four limit state

4.2 Parametric vulnerability functions

It was observed above that the vulnerability curves are distinct but have common features. It was further concluded that the overstrength ratio is a significant parameter influencing the vulnerability curves (it should be noted that the deformational capacity of the four bridges is similar, since they are all detailed to modern practice. In cases where this is not true, the deformation or rotation ductility of pier may be another influential parameter). It was therefore decided to attempt to define a ‘generic’ vulnerability curve and scaling factors that are related to the overstrength parameter. The application of the scaling factors would enable the individual structure vulnerability functions to be retrieved.

First the average of damage probability points at each PGA level is obtained and a cubic spline is fitted to the resulting points. Due to the differences in shapes of curves for different limit states, sets of curves for each LS is dealt with separately. The cubic spline and the analytically-derived values for each bridge at each limit state are presented in Figs. 10, 11, 12 and 13.

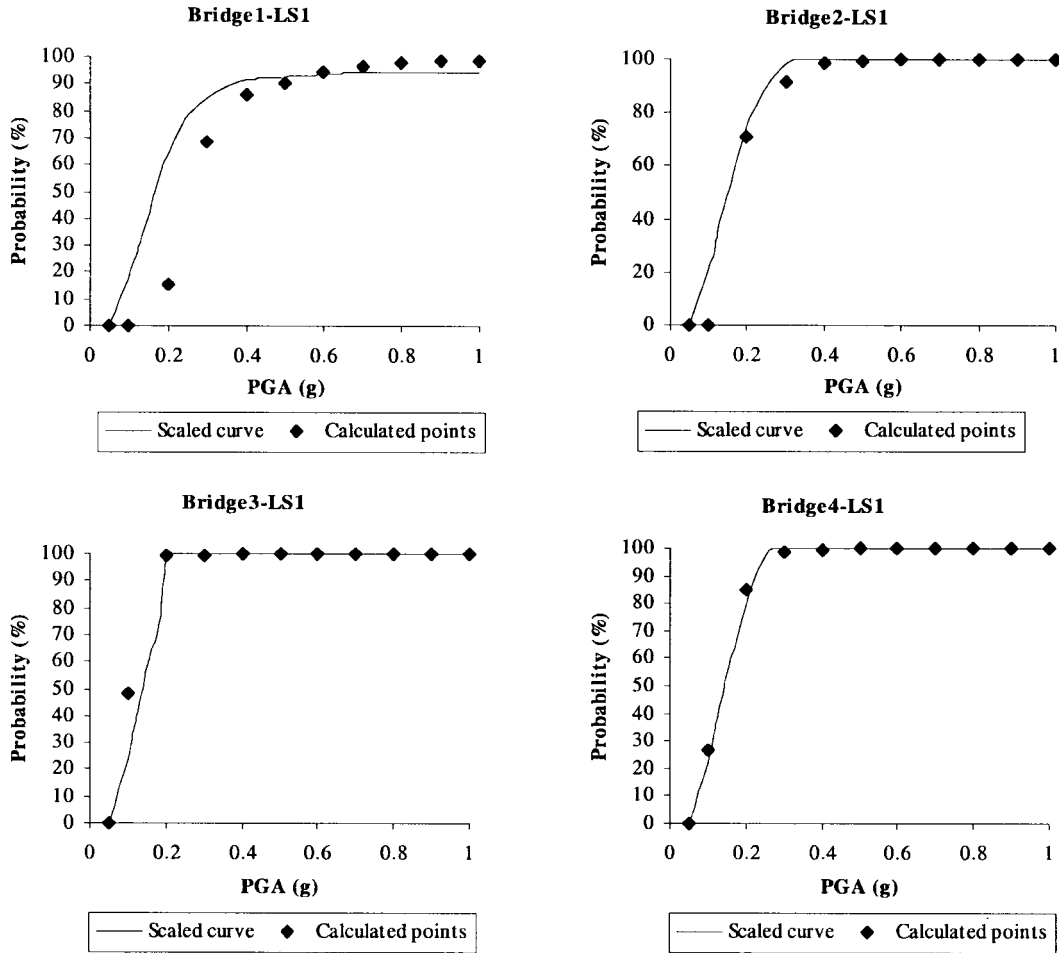


Fig. 10 Curve fitting for the first limit state

In general the shape of the vulnerability curves is well-represented by the cubic spline interpolation. In all cases it seems that a single curve can represent the general pattern of the vulnerability curves of all the different configurations. Some significant differences are observed in the vulnerability curves of Bridge 1. This is mainly due to the fact that these usually start from higher values of PGA. Since the curve is just multiplied by a constant factor and starts from lower values of PGA, it cannot follow very closely the vulnerability curve but instead is parallel to it and fits in the higher values of PGA. The results collectively confirm the feasibility of the procedure.

In Table 20 the multipliers that were used for each case are reported. It is noteworthy that the factors for the three limit states that refer to higher damage levels are practically constant. This indicates that there may be a correlation between vulnerability curves for different limit states for the same structure that can be further parameterized. This is, however, not attempted here.

The curves derived from this simple procedure are approximations of the analytically-derived curves. The errors for each case are reported in Tables 21 and 22. The error in some points is high but the main purpose is to approximate the shape of the curves and not to estimate the exact

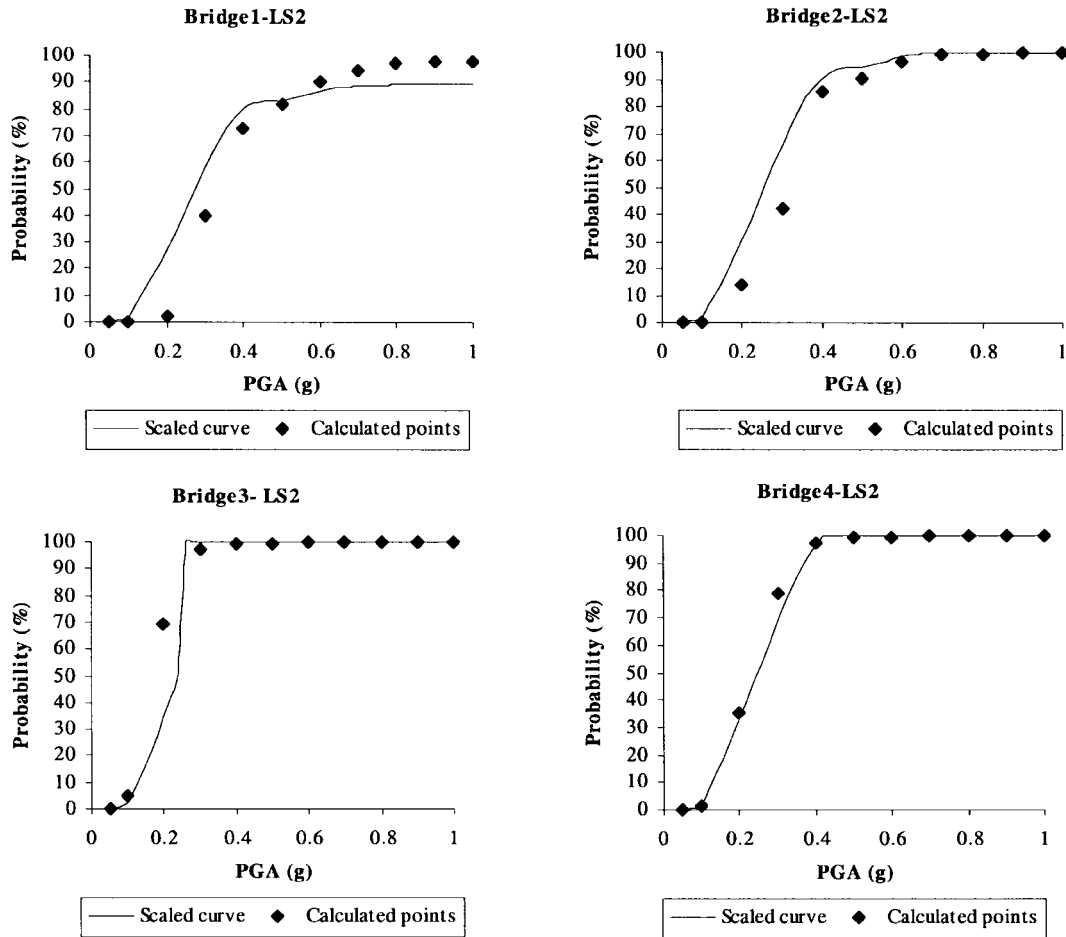


Fig. 11 Curve fitting for the second limit state

analytical values. Taking into account the uncertainty involved in validating vulnerability curves by comparison to field data, the results are adequately representative of the analytical values.

The multipliers used to derive one curve from another may be related to structural characteristics of the bridge such as the ductility or the overstrength ratio. As previously mentioned, member detailing is the same in all cases, hence deformation ductility is expected to be comparable. This is verified by the results of the pushover analyses presented in Table 19. Assuming that the overstrength parameter is the single most influential variable in this study, an attempt is made at relating the vulnerability curves scaling factor to the overstrength parameter, as described below.

For each pair of bridges the difference in the overstrength parameter and the corresponding scaling factors for the curves of the two bridges are estimated and reported in Table 23. It is observed that in two cases there is almost identical change in the overstrength ratio. In these two cases the corresponding multipliers are almost identical, indicating the possibility of relating the two quantities. Furthermore, it is observed that the two quantities vary in the same direction (increase or reduction).

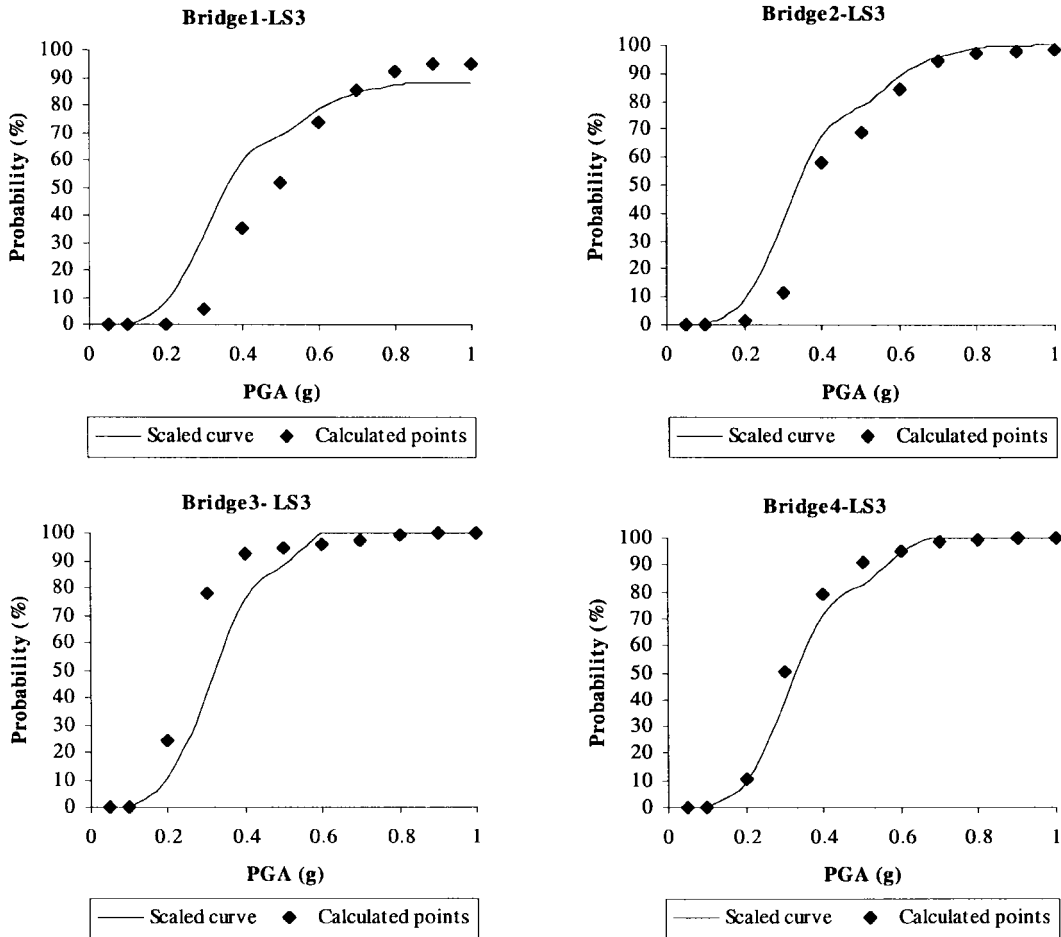


Fig. 12 Curve fitting for the third limit state

The strong correlation between overstrength and curve multiplier is emphasised by the results shown in Table 20. This indicates that for the three limit states that correspond to higher damage levels (LS 2, 3 and 4) a constant set of curve multipliers exist. In Fig. 14 the variation of the overstrength parameter is plotted versus the curve multiplier (scaling factor), indicating linear interdependence.

It is therefore straightforward to derive vulnerability curves for a bridge with given configuration once the curves for a different bridge have been derived. For this limited study of four bridges, the linear best-fit curves given in Eq. (14) below may be employed.

$$\begin{aligned}
 \text{LS 1:} \quad & k = 0.076 \cdot x + 0.9 \\
 \text{LS 2-3-4:} \quad & k = 0.0053 \cdot x + 0.96
 \end{aligned}
 \tag{14}$$

where k is the required scaling factor and x is the change in the overstrength ratio (%).

The emphasis in this part of the current study is on the ‘feasibility’ as opposed to the ‘accuracy’ of the proposed approach. It is fully recognised that many more bridges belonging to clearly defined

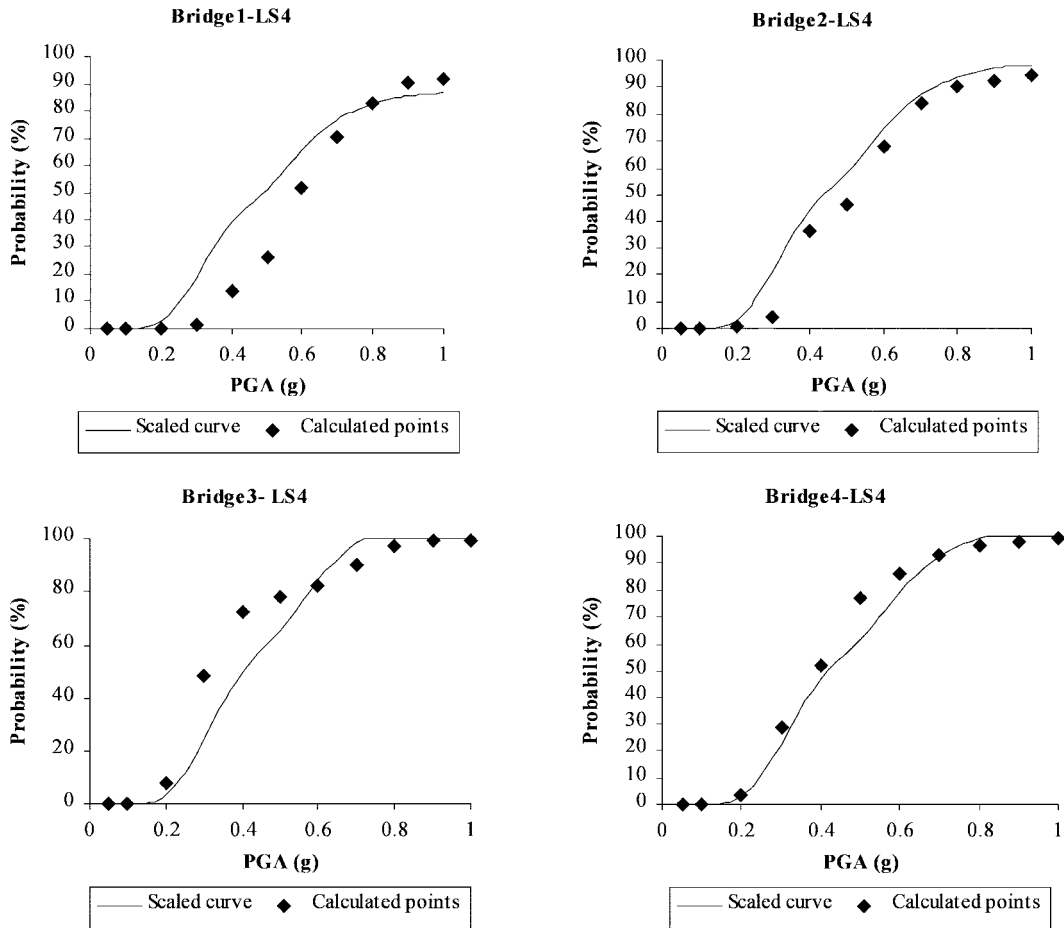


Fig. 13 Curve fitting for the fourth limit state

Table 20 Factors used for the curve fitting for each bridge at each limit state

	Bridge 1	Bridge 2	Bridge 3	Bridge 4
LS1	0.95	1.1	1.27	1.18
LS2	0.9	1.02	1.15	1.08
LS3	0.9	1.02	1.15	1.08
LS4	0.9	1.02	1.15	1.08

categories should be studied before a generally-applicable ‘generic’ vulnerability functions are derived alongside scaling factors, given as functional representations of bridge strength and deformational characteristics. However, the results given above are clearly promising and the simplicity of the procedure is rather appealing.

Table 21 Differences between analytically-derived and parameterized vulnerability curves B1-B2

PGA	Bridge 1				Bridge 2			
	LS1	LS2	LS3	LS4	LS1	LS2	LS3	LS4
0.1	1	1	1	1	1	1	1	1
0.2	3.190	13.128	689.925	591.211	0.048	1.248	4.850	5.580
0.3	0.238	0.465	5.069	15.169	0.075	0.553	2.141	4.253
0.4	0.059	0.097	0.692	1.848	0.069	0.057	0.157	0.235
0.5	0.024	0.022	0.325	0.959	0.078	0.044	0.137	0.244
0.6	0.010	0.038	0.062	0.275	0.086	0.020	0.052	0.096
0.7	0.026	0.061	0.008	0.087	0.092	0.008	0.016	0.042
0.8	0.036	0.080	0.053	0.005	0.095	0.004	0.020	0.036
0.9	0.038	0.085	0.073	0.057	0.096	0.003	0.024	0.050
1	0.038	0.085	0.071	0.058	0.096	0.001	0.019	0.041

Table 22 Differences between analytically-derived and parameterized vulnerability curves B3-B4

PGA	Bridge 3				Bridge 4			
	LS1	LS2	LS3	LS4	LS1	LS2	LS3	LS4
0.1	0.509	0.629	0.640	1	0.167	0.196	0.391	1
0.2	0.010	0.500	0.567	0.560	0.062	0.086	0.074	0.123
0.3	0.010	0.031	0.464	0.512	0.017	0.116	0.218	0.226
0.4	0.000	0.006	0.175	0.311	0.005	0.013	0.094	0.092
0.5	0.000	0.004	0.067	0.158	0.000	0.008	0.093	0.203
0.6	0.000	0.003	0.042	0.025	0.000	0.004	0.005	0.079
0.7	0.000	0.002	0.025	0.091	0.000	0.001	0.013	0.010
0.8	0.000	0.001	0.004	0.026	0.000	0.000	0.006	0.030
0.9	0.000	0.000	0.001	0.009	0.000	0.000	0.003	0.020
1	0.000	0.000	0.000	0.004	0.000	0.000	0.001	0.007

Table 23 Ratio of the multipliers according to the difference of overstrength

	Difference of the Overstrength ratio (%)	LS1	LS2	LS3	LS4
Bridge 2-Bridge 4	16	1.03	1.06	1.06	1.06
Bridge 4-Bridge 3	23	1.07	1.065	1.065	1.065
Bridge 1-Bridge 2	35	1.16	1.13	1.13	1.13
Bridge 2-Bridge 3	35	1.16	1.13	1.13	1.13
Bridge 1-Bridge 4	45	1.24	1.2	1.2	1.2
Bridge 1-Bridge 3	57	1.34	1.28	1.28	1.28

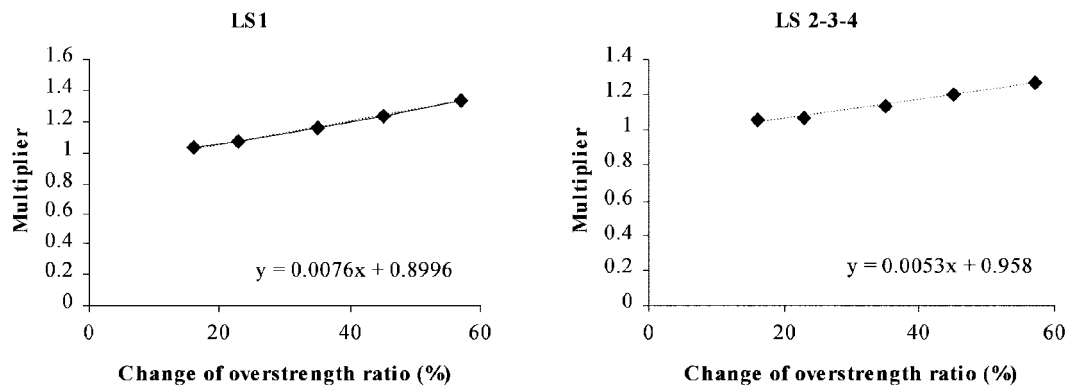


Fig. 14 Correlation of change of overstrength ratio with the factors that give the corresponding vulnerability curve

5. Conclusions

The paper presents three contributions to the important and fast-developing subject of vulnerability analysis of bridges. First, two observational data banks from two previous earthquakes presented by Basöz *et al.* (1999) and Yamazaki *et al.* (1999) are used to derive a set of observationally-based vulnerability curves. Next, a simple, transparent and pragmatic analytical procedure to derive vulnerability functions for reinforced concrete bridges is outlined. The procedure utilises recent developments in deformation-based assessment. The selected limit states provide a clear correspondence between local deformation quantities (strain) and structure-level measures (displacements). Four limit states are employed, ranging from no damage to severe levels of distress. In arriving at a complete procedure a number of assumptions were made and justified. It is however emphasised that considerable room for further development exists. Moreover, of the analytical curves comparison with observational data (Northridge 1994 and Kobe 1995) vulnerability functions provides a degree of confidence in the analytical results. Based on the acceptable level of correlation between analytical and observational functions derived in this work, the curves are feasible for use in seismic damage assessment.

The third contribution to vulnerability analysis presented in this paper is a simple procedure to derive vulnerability curves for one structure from another whilst bypassing simulation and analysis requirements. In this study, the vulnerability functions are parameterized using the overstrength ratio (ratio of available-to-design base shear) of four bridges that belong to the same class of bridge but have different geometric, hence strength, properties. Simple relationships were derived to establish vulnerability functions of one bridge from those of another once the overstrength ratio was obtained from pushover analysis. One of the main applications of this procedure is in large projects where many bridges have the same basic configuration with some changes in member sizes, spans and pier heights. Given the vulnerability curves of one bridge, the proposed relationships could be used to derive vulnerability functions for the rest of the group directly.

Acknowledgements

The authors are grateful to EQE International Ltd (UK) and Egnatia Othos AE, Greece, for

funding part of the above study. The work described above was undertaken during the tenure of the primary author at Imperial College, London, UK. The final version of the paper was developed with the support of the Mid-America Earthquake Center researchers and facilities. The Mid-America Earthquake (MAE) Center is funded by the US National Science Foundation under grant reference EEC-9701785.

References

- ATC 6-2 (1983), "Seismic retrofitting guidelines for highway bridges", *Applied Technology Council*, Redwood City, California; also FHWA/RD 83/007 report.
- Basöz, N.I. and Kiremidjian, A.S. (1997), "Evaluation of bridge damage data from the 1994 Northridge, CA earthquake", *NCEER-97-0005, Workshop on Earthquake Engineering Frontiers in Transportation Facilities*, 167-181.
- Basöz, N.I., Kiremidjian, A.S. and Straser, E. (1994), "Prioritization of bridges for seismic retrofitting", *Fifth U.S. National Conf. on Earthq. Eng.*, 881-890.
- Basöz, N.I., Kiremidjian, A.S. and King, S.A. (1999), "Statistical analysis of bridge damage data from the 1994 Northridge, CA, earthquake", *Earthquake Spectra*, **15**, 25-54.
- Eurocode 8 (1994), "Design provision for earthquake resistance of structures", *ENV 1998-1, CEN, Brussels*.
- Ghobarah, A. and Ali, H.M. (1988), "Seismic performance of highway bridges", *Eng. Struct.*, **10**, 157-166.
- Hognestad, E. (1951), "A study of combined bending and axial load in reinforced concrete members", *University of Illinois Bulletin*, Bulletin Series No 399.
- Hoshikuma, J., Kawashima, K., Nagaya, K. and Taylor, A.W. (1997), "Stress-strain model for confined reinforced concrete in bridge piers", *J. Struct. Eng.*, ASCE, 624-633.
- Izzudin, B.I. and Elnashai, A.S. (1989), "ADAPTIC: A program for the adaptive large displacement inelastic dynamic analysis of frames", *ESEE Report no. 89-7, Imperial College, London, UK*.
- Kappos, A., Chryssanthopoulos, M.K. and Dymiotis, C. (1998), "Probabilistic assessment of European seismic design practice for confined members", *European Earthq. Eng.*, **12**, 38-51.
- Kawashima, K. and Unjoh, S. (1997), "The damage of highway bridges in the 1995 Hyogo-Ken Nanbu earthquake and its impact on Japanese seismic design", *J. Earthq. Eng.*, **1**(3), 505-543.
- Kent, D.C. and Park, R. (1971), "Flexural members with confined concrete", *Proceeding ASCE*, **97**, 1969-1990.
- Mattock, A.H., Kizir, L.B. and Hognestad, E. (1961), "Rectangular concrete stress distribution in ultimate strength design", *J. ACI*, **57**, 875-826.
- Ming, J.Y., Lui, E.M. and Liu, Y. (2001), "Dynamic response of skew highway bridges", *J. Earthq. Eng.*, **5**, 205-223.
- Mirza, S.A., Hatzinikolas, M. and MacGregor, J.G. (1979), "Statistical descriptions of strength of concrete", *ASCE J. the Struct. Div.*, **105**, 1021-1037.
- Park, R. and Paulay, T. (1975), *Reinforced Concrete Structures*, Wiley-Interscience.
- Paulay, T. and Priestley, M.J.N. (1992), *Seismic Design of Reinforced Concrete and Masonry Buildings*, Wiley-Interscience.
- Pipa, M. and Carvalho, E.C. (1995), "Reinforcing steel characteristics for earthquake resistant structures", *10th European Conf. on Earthq. Eng.*, 2887-2892.
- Priestley, M.J.N., Seible, F. and Calvi, G.M. (1996), *Seismic Design and Retrofit of Bridges*, Wiley-Interscience.
- Rossetto, T. and Elnashai, A.S. (2003), "Derivation of vulnerability functions for European-type RC structures based on observational data", *Engineering Structures*, Accepted for Publication February.
- Shinozuka, M., Feng, M.Q., Kim, H-K. and Kim, S-H. (2000), "Nonlinear static procedures for fragility curve development", *J. Eng. Mech.*, ASCE, **126**, 1287-1295.
- Yamazaki, F., Onishi, J. and Tayama, S. (1999), "Earthquake damage assessment of expressway structure in Japan", *Asian-Pacific Symposium on Structural Reliability and its Applications*, 1-10.